

Dichoptic Multifocal Pupillography Reveals Afferent Visual Field Defects in Early Type 2 Diabetes

Andrew Bell,¹ Andrew C. James,¹ Maria Kolic,¹ Rohan W. Essex,² and Ted Maddess¹

PURPOSE. Multifocal pupillographic perimetry was used to examine differences in the visual fields of 23 subjects with early type 2 diabetes (T2D) and 23 age- and sex-matched control subjects.

METHODS. Independent stimuli were delivered to 44 regions of each eye while pupil responses were recorded with infrared cameras. The stimuli were presented in 8 segments of 30 seconds, and both eyes of each subject were tested twice. The direct and consensual responses provided 88 responses per eye. The diagnostic power of the method was then examined by applying receiver operator analysis to the peak regional contraction amplitudes, time to peaks, and linear combinations of those.

RESULTS. Dichoptic multifocal pupillography provided response amplitudes with a median z -score of 2.63 ± 0.26 (SE). The diagnostic performance (expressed as areas under ROC plots) of the eight subjects (32 fields) who had had T2D for at least 10 years was 0.87 ± 0.06 (mean \pm SE) for response amplitude deviations from normative data, rising to 0.95 ± 0.04 when between-eye symmetry was considered. Mean pupil size did not have diagnostic power. Comparison of direct and consensual response fields indicated that the observed localized field defects were afferent.

CONCLUSIONS. Reasonable diagnostic power was obtained, especially for the 16 eyes that had had T2D for more than 10 years, inferring that even in the near absence of visible diabetic retinopathy, some retinal damage had been sustained. This result, if confirmed in a wider group, suggests that the method may be clinically useful in screening for early damage to the retina in T2D diabetes. (*Invest Ophthalmol Vis Sci* 2010;51:602–608) DOI:10.1167/iovs.09-3659

The prevalence of type 2 diabetes (T2D) is rising,¹ T2D is the greatest cause of vision loss among people of working age.² With good metabolic control, however, the risk of disease of the retinal microvasculature and the associated sight-threatening complications can be reduced.³ The earliest visible sign is nonproliferative diabetic retinopathy (NPDR).⁴ Several groups report that perimetry can identify retinal changes

caused by diabetes, before retinopathy occurs.^{5–11} The time elapsed since diagnosis of the disease appears to be a significant factor in determining the perimetric mean deviation (MD).¹¹ A more rapid and objective perimetric test for retinal damage due to T2D may therefore help reduce future vision loss.

When undergoing automated perimetry, patients with glaucoma^{12–14} or optic neuritis¹⁵ commonly have rates of fixation losses, false positives, and false negatives that are outside the manufacturer's specified limits; the proportion of such subjects can run to 10% or more.^{12–15} These subjects are generally excluded from clinical studies, but this practice can yield sensitivities and specificities that are less relevant in the clinic. From the perspective of T2D, patients with macular edema display poor fixation.¹⁶

In working toward objective tests of visual fields, multifocal methods appear attractive because they test many parts of the visual field concurrently.¹⁷ Several studies have shown that multifocal (mf)ERGs can detect damage in mildly affected persons with diabetics.^{18–21} Also promising is dichoptic stimulation, which involves concurrent stimulation of both eyes with independent stimuli, which has been shown to work with mfVEPs,^{22–26} and has been applied in clinical studies.^{27,28} A drawback is that mfVEPs can take more than 30 minutes to set up and execute.²⁹

Perimetry based on pupillography, which requires little setup time, has been demonstrated.^{30,31} Three studies have examined multifocal pupillographic objective perimetry (mfPOP) (Sutter EE, et al. *IOVS* 1996;37:ARVO Abstract 3157).^{32,33}

Unfortunately, mfPOP methods have, to date, generated low signal-to-noise ratios (SNRs), and thus have required long presentation times. Video monitoring of the eyes, however, opens up the possibility of accurately monitoring fixation.

Recent work from this laboratory demonstrates that the SNRs and test times of mfVEPs can be improved by the use of sparse stimuli (James AC, et al. *IOVS* 2005;46:ARVO E-Abstract 3602).^{23–25,27} Sparse stimuli have few neighboring regions, spatially or temporally. Sparse multifocal dichoptic stimuli and pupillography have been used to assess glaucomatous fields.³⁴ The focus of this study was the first application of these combined methods to T2D.

METHODS

Subjects

We recruited 23 patients (12 men, 11 women; mean age, 58.0 ± 6.9 [SD] years) who a diagnosis of T2D. They had visual acuity better than 6/12, normal intraocular pressure, and no ocular surgery. They were age- and sex-matched with 23 normal subjects (mean age, 59.7 ± 5.6 years), who were given a thorough eye examination involving applanation tonometry, OCT, FDT C-20 field tests, SWAP, and 24-2 SITA Fast tests (Humphrey Field Analyzer; Carl Zeiss Meditec, Inc., Dublin, CA). Their records were examined by an ophthalmologist (RWE). The patients had no apparent visual dysfunction. Most (21/23) had no retinopathy, two had mild NPDR. Other inclusion criteria were that all

From the ¹ARC Centre of Excellence in Vision Science and Centre for Visual Sciences, Research School of Biology, The Australian National University, Canberra, ACT, Australia; and the ²Ophthalmology Department, The Canberra Hospital, Canberra, ACT, Australia.

Supported by the Australian Research Council (ARC) through the ARC Centre of Excellence in Vision Science (CE0561903), AusIndustry, and Seeing Machines.

Submitted for publication March 4, 2009; revised June 26 and July 17, 2009; accepted July 17, 2009.

Disclosure: **A. Bell**, Seeing Machines (F, C); **A.C. James**, Seeing Machines (F, I, C, P, R); **M. Kolic**, Seeing Machines (F, R); **R.W. Essex**, None; **T. Maddess**, Seeing Machines (F, I, C, P, R)

Corresponding author: Ted Maddess, ARC Centre of Excellence in Vision Science and Centre for Visual Sciences, The Australian National University, Canberra, ACT 0200, Australia; ted.maddess@anu.edu.au.

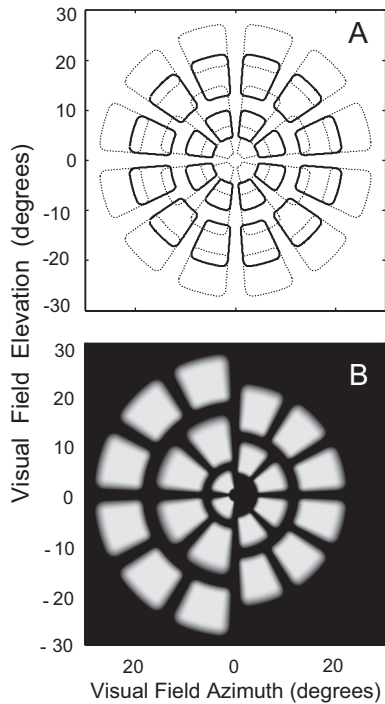


FIGURE 1. The dartboard arrangement of the 44 blurred stimuli (11 per quadrant). (A) Contour plots at half height of the regions showing the degree of overlap of the regions. Most of the overlap is in the blurred skirts of the patches. Note that the stimuli do not overlap the horizontal and vertical meridians. In practice, the stimuli never overlapped in time or space during a presentation. (B) Composite image of the stimulus patches; *left* side showing six per quadrant and the *right* side the remaining five.

subjects had distance refraction $< \pm 6$ D, < 2 D of cylinder, and a pupil ≥ 2.5 mm in the test room. All participants gave informed written consent and were tested twice, 2 to 4 weeks apart. The study conformed with the Declaration of Helsinki.

Stimuli and Recording

Subjects were tested with a prototype version of a field analyzer (TrueField Analyzer; Seeing Machines, Braddon, Australia). Seated in a room with subdued lighting, the subjects were instructed to fixate a central red cross arranged to appear at infinity on a stereoscopic pair of LCD displays refreshed at 60 frames/s. Visual stimulation was supplied to both eyes independently as 44 transiently presented (33 ms)

yellow elements extending to 30° eccentricity (Fig. 1). The mean presentation rate of each pseudorandomly presented element was 1 per second. Each element was presented with a central luminance of 290 cd/m² against a stereoscopically fused and stable background pattern of 10 cd/m². The stimuli were arranged to be spatially and temporally sparse (James AC, et al. *IOVS* 2005;46:ARVO E-Abstract 3602).²³ Each test lasted for 4 minutes, divided into eight segments of 30 seconds. The stimulus elements contained no spatial frequencies above 2 cyc/deg, thereby providing tolerance to refractive error. Corrective lenses, to the nearest 1.5 D spherical equivalent, were fitted when needed.

Pupil responses were recorded by infrared video cameras under infrared illumination. Pupil diameter was monitored 30 times/s by fitting a circle to the lower three fourths of the pupil, providing some tolerance to ptosis. Data recorded during blinks and fixation losses were deleted. If data acquisition fell below 85% within any 30-second segment, it was repeated. The multifocal analysis algorithm used a multiple regression method,³⁵ rather than cross correlation.³⁶

Analysis

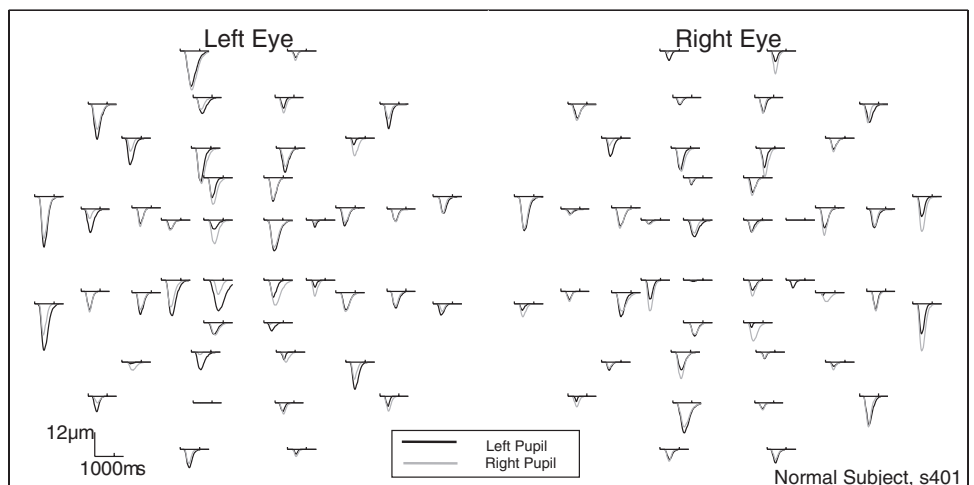
All analyses were performed with commercial software (MatLab; The Mathworks, Natick, MA). Pupil size was normalized to the mean value of a trend line through the 240 seconds of pupil diameter data of each test. Thus, the multifocal responses were relative responses compared with a normalized diameter of 1 (dimensionless). For convenience, normalized data were multiplied by 3.5 mm, the mean pupil size of the subjects. The resulting peak scaled response amplitudes are referred to as standardized amplitudes (AmpStd).

The data produced by the TrueField device are effectively the mean response to the transient stimuli presented at each test region (e.g., Fig. 2). The response waveforms were fitted to the log-normal function $A \exp[-(\ln(t/t_p)/\sigma)^2]$, where A is the peak amplitude, t_p is the time to peak (PeakTime), and σ defines the width of the response. The direct and consensual responses for each test region resulted in $44 \times 2 \times 2 = 176$ response waveforms per test.

Diagnostic power was assessed by receiver operator characteristic (ROC) plots, summarized as the area under the curve (AUC). Standard errors in the AUCs were also calculated.³⁷ The ROC analysis was based on regional deviations from the normative data, not unlike the total deviations (TDs) of a perimeter. The steps in computing these deviations were:

1. Select the parameter to be analyzed (e.g., standardized amplitude).
2. Pool the direct and consensual visual field data. Pooling was achieved by selecting the direct or consensual field with the largest median z-score (i.e., the more reliably measured field of the two).

FIGURE 2. Pupil response waveforms. Each stimulus produces pupil contractions, as shown by the downward-dipping response waveforms in the example shown here (normal subject s401). Each stimulus produces responses in the same eye (the direct response) and in the opposite eye (the consensual response). Subsequent analysis focused on three main factors: the magnitude of each contraction, the time to peak, and a linear combination of the two. The mean percentage of valid data in the 30-second test periods across all subjects and repeats was $98.0\% \pm 2.5\%$ (SD).



3. Compute the normative data via a multivariate linear model that fitted the means for every field location of the normal subjects (including a constant offset for the women).
4. Subtract the fields of all subjects from the normative data to create deviations from normal at each field location.
5. Optionally, compute the visual field asymmetry between eyes by replacing the deviations with the absolute value of the differences between left and right eye field locations.
6. Optionally, repeat steps 1 to 5 for a second parameter (e.g., PeakTime), creating a second set of deviations. Then form a linear combination, or deviation score, of the two forms of deviations based on a Fisher's linear discriminant function³⁸ which best separated the normal subjects and patients. This method defines a two-element vector with coefficients $w_i = S^{-1}(m_1 - m_2)$, where the m_i are the means of the parameters, and S is the 2×2 pooled covariance matrix. The scores are then the dot product $w \cdot x_i$, where x_i is a two-element vector containing each pairing of deviations for each field location.
7. Transform the final deviations to z -scores, permitting transformation to probabilities that individual field locations differ from the normative data. For step 7, the final deviations were transformed into equivalent probabilities according to the empiric distribution of deviation values over the normative data, separately for each visual field region. The transformation was achieved by interpolation of the mapping from empiric distribution of normative values to equivalent standard normal quantiles, with linear extrapolation, and then mapping to equivalent probability values.

Figure 3 illustrates the outcome of this process for one subject. Two analyses were performed for Figure 3: one in which at step 2 only the left pupil data were used (Figs. 3A, 3B), and a second using only the right pupil data (Figs. 3C, 3D). In this particular subject, the median z -score at step 2 was 2.67 for the left pupil and 2.57 for the right; therefore, in the usual analysis the fields from the left pupil would have been selected for ROC analysis. It may be supposed that taking the mean across pupils would be more reliable; however, most of the noise is on the efferent pathways and therefore is correlated between the

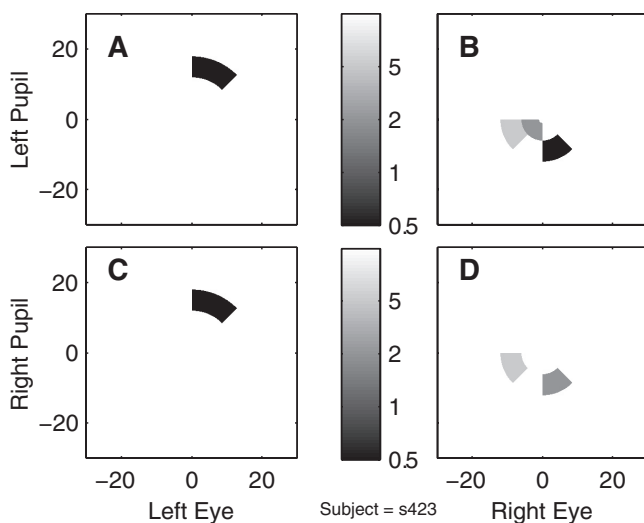


FIGURE 3. An illustration of the outcome of the process of computing deviations from normal responses amplitudes. The deviations were expressed as z -scores, which have here been transformed to percent probabilities that a given field location is normal (density scale at right of each plot), the lowest displayed being $P \leq 0.5\%$. The z -score deviations were the basis of the ROC analysis. Data were computed on the responses of the subject's (A, B) left and (C, D) right pupils. In this example, it is clear that the significant local defects must be afferent in origin, because the responses follow the retinal pattern, irrespective of which pupil is being measured.

TABLE 1. Overall t -Statistics

	Normal Subjects	T2D Subjects
AmpStd	2.66 ± 1.32	2.61 ± 1.20
Peak Time	22.8 ± 11.3	22.2 ± 11.2

Data indicating the median significance of two key response variables, AmpStd and PeakTime (time to reach maximum contraction). Data are expressed as the mean ± SE.

pupils, and so averaging fields across pupils adds no value. One advantage is that only one functional pupil is required.

RESULTS

Examples of pupil contraction waveforms are shown in Figure 2, where each response waveform is placed at a position corresponding to the visual field stimulus region that evoked it. The measurements of AmpStd and PeakTime from the 176 response waveforms recorded for each subject and repeat were quite accurate, yielding median t -statistics between 2.61 and 22.8 (Table 1).

We used multivariate linear models to examine what factors, on average, significantly determine AmpStd or PeakTime. The models contained a constant, or reference, value and then coefficients for factors that were fitted as contrasts to the reference value. Hence, for these factors, the t -statistics and P -values refer to the significance of the difference from the reference condition. In Tables 2 and 3 the reference can be thought of as the grand mean across direct responses of male subjects. In other models, factors for each region were also fitted (Figs. 4, 5).

Table 2 shows the result of fitting a model for AmpStd transformed into decibels. Log transformation was appropriate because the main effects appeared to be multiplicative. Table 2 shows that, on average, the direct responses of the pupils of the male subjects (the reference condition) contracted by 10.4 ± 0.1 dB (mean ± SE) in response to a stimulus (i.e., $10.96 \mu\text{m}$ for a 3.5-mm pupil). It also shows that the pupils of the women contracted by an additional 0.43 ± 0.04 dB (10.4% more); the consensual response was 0.4 ± 0.1 dB (9.65%) smaller than the direct response; and diabetic subjects had larger pupil responses by 0.29 ± 0.04 dB (6.91%).

A more detailed picture emerged when factors for each region were included in the model. Figure 4 shows the resulting mean region-by-region response amplitudes in normal subjects (Fig. 4A), and the additional mean deviations of the diabetic subjects (Fig. 4B). Data for the left and right eyes were combined so that nasal visual field regions corresponded to that of a left eye. As suggested by Figure 2, the mean temporal visual field responses were larger than those from the nasal field (Fig. 4A). The 11 smallest mean responses (darkest re-

TABLE 2. Independent Effects on Pupil Contraction Amplitudes Estimated by a Multivariate Linear Model

Variable	dB	SE	t -Stat.	P
Reference	10.4	0.13	78.1	5.3E-315
Consensual	-0.43	0.04	-9.98	2.20E-23
Female	0.43	0.04	10.0	1.40E-23
T2D	0.29	0.04	6.85	7.50E-12

The reference (grand mean of direct responses of male subjects) response amplitude was 10.4 dB, and the three other factors show deviations from that value (positive values represent an increase), and the significances of those deviations from the reference condition.

TABLE 3. Independent Effects on the Time to Peak Contraction

Variable	ms	SE	t-Stat.	P
Reference	466.2	2.47	188.5	1.00E-307
Consensual	0.74	0.65	1.13	2.60E-01
Female	-12.7	0.65	-19.42	4.90E-83
T2D	5.00	0.65	7.66	2.00E-14

The average delay is 466.2 ms. Note that, unlike response amplitude, there is no significant effect of consensual response ($P = 0.26$).

gions) of the mean diabetic deviations (Fig. 4B) were not significantly different than no deviation, $t = 1.07 \pm 0.06$ (mean \pm SE). This mean effect does not rule out individual fields' having significant deviations from normal (e.g., Fig. 3). By contrast, the 33 regions with deviations corresponding to larger than normal responses (brightest regions) were, on average, significant ($t = 2.12 \pm 0.12$), consistent with the mean effect of T2D in Table 2.

The regional delays were also informative (Figs. 5A, 5B). Here, the increased mean delays of T2D subjects are shown as lighter grays. The five most delayed (lightest regions) of Figure 5B reached marginal (one-tailed) significance ($P < 0.05$, $t = 1.82 \pm 0.13$). Similar results were found when linear models

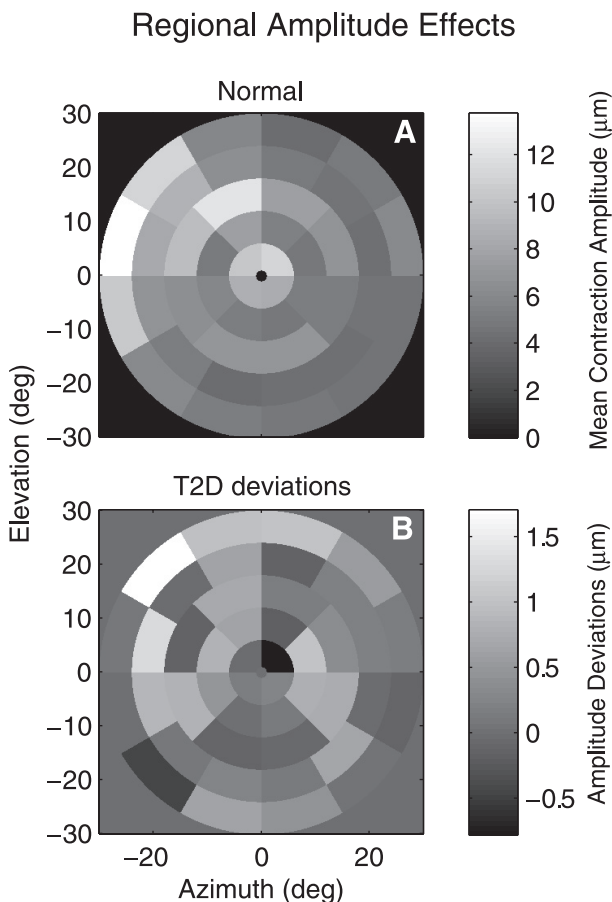


FIGURE 4. Region-by-region mean pupil contraction factors. The average contractions in (A) normal and (B) diabetic subjects, expressed as mean deviations from the normal data in (A). Responses from both eyes have been combined and presented as if they were all from left eyes; hence, the nasal field is on the right. For reference, the gray level corresponding to 0 deviation from normal subjects is set as the background of Figure 3B. There are 33 mainly peripheral regions in (B) that are significantly larger than normal ($t > 2.0$).

Regional Delay Effects

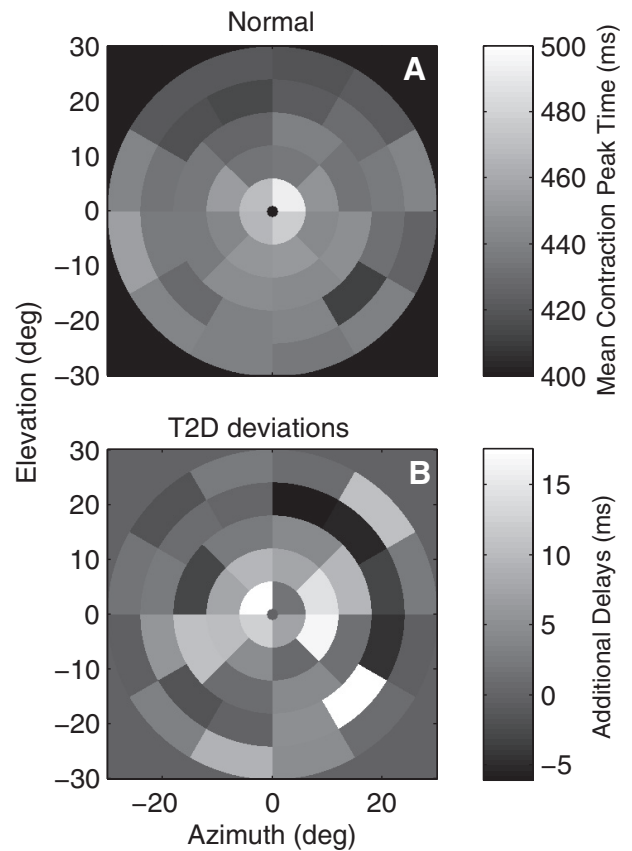


FIGURE 5. Region-by-region mean pupil contraction delays. The layout is as in Figure 4, except PeakTime is considered and longer delays are depicted in lighter gray. (A) The normal subjects show a gradient of increasing delay from superior to inferior field. (B) The central five most-delayed regions of the mean T2D data are only marginally significant.

were constructed in which only the mean effect of T2D across regions was considered, rather than region-wise factors (Table 3). The average value for the men was 466 ± 2 ms, whereas the women were 12.7 ± 0.7 ms quicker. T2D increased the response delay by 5.0 ± 0.7 ms on average (cf. Fig. 5B). It is worth noting that no significant age effects were found for either delay or amplitude, perhaps reflecting the narrow sample range.

We next examined the diagnostic power of visual field deviations from the normative data for individual fields by using receiver operator characteristic (ROC) analysis.³⁹ Variables such as AmpStd, PeakTime, response width, and absolute pupil size were considered. We also examined deviation scores obtained from linear discriminant models that combined deviations obtained from two parameters and between-eye asymmetry.

Examples of the result of the deviation calculation are shown in Figure 3, where separate fields were derived for data arising from the left (Figs. 3A, 3B) and right (Figs. 3C, 3D) pupils. The z-score deviations were transformed to probabilities that a given visual field location is normal, not unlike the TDs of a perimeter. The observed local deviations must be due to afferent (not efferent) effects because they are consistent with the eye of origin rather than the pupil from which the fields were measured. To confirm this conclusion across all patients, we took the between-eye and between-pupil differ-

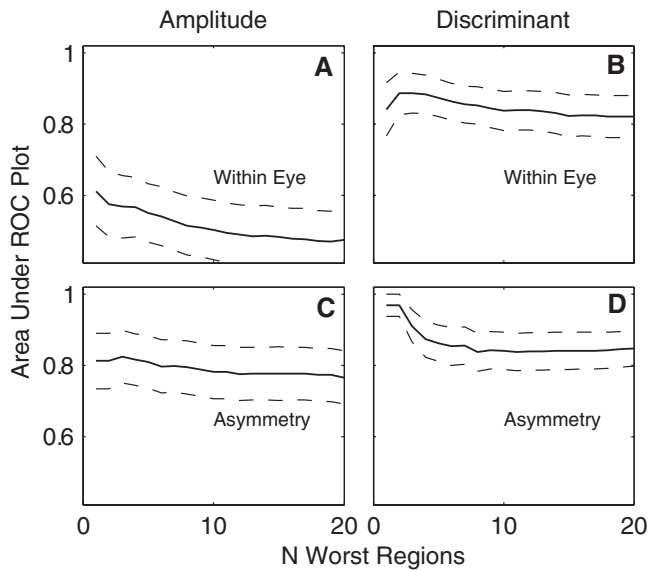


FIGURE 6. ROC area (AUC) \pm SE plotted as a function of the mean of the n -worst regions in the normal subjects compared with the n -worst regions in the patients. The two variables considered are AmpStd (A, C) and the discriminant function combining amplitude and delay (B, D). The within-eye case examines deviations from mean normal data for each visual field region of each eye. In the asymmetry case, the differences between a subject's left and right fields at each location are considered.

ences for every location in every field. Consistent with afferent effects, the between-eye differences were significantly ($t = 26.3$) smaller (by 0.45 z -score units) than were the between-pupil differences.

In distinguishing the deviations of diabetic subjects from normal ones, it was informative to assign the diabetics to one of three *severity ratings*. To create these severity ratings, we examined five parameters related to diabetes: the average percent HbA1c level over the past 2 years; number of diabetic medications currently used; mean and pattern deviations on a companion FDT C20 test; and the number of years that T2D had been diagnosed. Each criterion level contained near-equal numbers of patients, and for each level we constructed ROC plots of sensitivity versus the false-

positive rate for recognizing a diabetic retina. One issue is how many field regions should be considered for making a diagnosis. To resolve this question, we created multiple ROC plots based on the n -worst deviating points in the fields of the diabetics and normal subjects. The number of compared regions, n , ranged from 1 to 20.

The results were encouraging, in that in those eight subjects with a diagnosis of T2D for more than 10 years (i.e., 32 fields = 8 subjects \times 2 eyes \times 2 repeats), we obtained percent AUCs of $88.0\% \pm 6.0\%$ (mean \pm SE, Fig. 6B), rising to $96.9\% \pm 3.0\%$ when between-eye asymmetry was considered (Fig. 6D). These values were obtained for n -worst = 2, and were a linear combination of AmpStd and PeakTime deviations based on a linear discriminant function. The weights for the linear combination were $w = (0.9992 \ 0.0406)$. Figure 6 indicates that between 1 and 3 largest deviations from normal (n -worst) were most diagnostic and had smaller or similar SE than any other n -worst. It is worth noting that the two subjects with mild NPDR in one eye were in the >10 -year group.

Table 4 shows the results for patients with a differing number of years of diagnosed T2D. Each entry in Table 4 is the mean of the percent AUC and SE obtained for n -worst = 1, 2, and 3. The AUCs increased fairly monotonically with increasing duration of disease. Unlike duration of disease, the other severity factors considered—HbA1c, number of medications, and FDT mean defects—did not produce useful AUCs.

The percent AUCs for response delay and width were not tabulated, as they were generally close to 50%. The best AUCs for delay were obtained in the patients with more than 10 years of T2D and were $75.5\% \pm 8.5\%$ in within-eye comparisons, and $69.7\% \pm 8.9\%$ in between-eye asymmetry, at an n -worst of 2. In addition, ROC analysis showed that absolute pupil diameter by itself did not provide any diagnostic power at any severity rating. This was not surprising, given that the average pupil size of the patients ($3420 \pm 776 \mu\text{m}$) was statistically indistinguishable ($P > 0.05$) from that of the normal subjects ($3275 \pm 637 \mu\text{m}$).

DISCUSSION

It is now becoming clear that, in addition to vascular damage, T2D causes degeneration of retinal glia and neurons early in the disease process,⁴⁰ so a method that can recognize this dysfunction could be clinically useful. Even in patients with

TABLE 4. Diagnostic Accuracy

Years	Eyes	Within Eye		Asymmetry		T2D Age Mean \pm SD
		AmpStd	Discrim	AmpStd	Discrim	
All	46	61.6 \pm 5.9	67.5 \pm 5.7	64.6 \pm 6.0	77.8 \pm 5.1	58.0 \pm 6.9
≤ 5	14	64.4 \pm 8.9	58.4 \pm 8.6	63.0 \pm 9.9	72.6 \pm 8.8	58.8 \pm 4.0
5 to 10	16	62.3 \pm 9.2	55.8 \pm 9.3	49.0 \pm 9.5	65.4 \pm 9.7	55.1 \pm 7.0
5 to 17	32	60.4 \pm 6.9	71.4 \pm 6.5	65.4 \pm 6.9	80.1 \pm 5.9	57.6 \pm 7.9
>10	16	58.5 \pm 9.2	87.1 \pm 6.3	81.7 \pm 7.6	94.9 \pm 3.6	60.1 \pm 8.3

Years, the number of years of diagnosed T2D; eyes, the number of eyes present in each T2D group (the number of fields entered into the ROC analysis was twice that number, given the two repeats). ROC data, based on within-eye deviations from the normative data (within eye). In each pair of data columns, the leftmost is based on the standardized peak contraction amplitudes (AmpStd) for each region, and the companion column is based on a linear discriminant function (Discrim) incorporating the peak amplitude and its delay; asymmetry, based on the differences between the deviations obtained in the left and right eyes for the same visual field location. For these table items, the AUC \pm SE were calculated for three cases: the single worst deviation, the two worst deviations, and the three worst deviations; the means of these three values and their SE are tabulated. AUCs $>75\%$ are shown in bold. The linear combination of amplitude and delay (Discrim) generally performed better than contraction amplitude alone, especially for between-eye asymmetry. The tabulated values in the bottom row (>10 y) are directly comparable to those in Figure 6. The rightmost column gives the mean \pm SD of the ages of the patients in each category.

T2D without serious retinopathy, evidence of retinal damage has been provided by perimetry⁸⁻¹⁰ and mfERGs.¹⁸⁻²¹

Nitta et al.¹¹ found, when considering a group of patients who had been diagnosed with T2D for between 0 and 10 years, that the effects of T2D observed with SWAP grew approximately linearly with time. As in that study, the duration of A1c levels was not correlated with SWAP, but fructosamine concentration reached near significance. Other studies indicate that both pre-NPDR⁷ and macula edema are picked up by SWAP¹⁰ and that it is more reliable than visual acuity in characterizing DR.⁸ It is worth noting that our yellow stimuli would drive blue/yellow chromatic mechanisms, notably the *yellow on/blue off* cone-mediated response of melanopsin-containing ganglion cells.⁴¹ Patients with 0 to 20 years of T2D, and mild to no retinopathy, have also shown significant changes on flicker perimetry.⁹

In the mfERG studies, response delay has been reported to have relatively high diagnostic value for diabetic retinopathy in patients who on visual examination have no (or only mild) DR.¹⁸⁻²¹ In the present case, response delay was less valuable than amplitude. Nevertheless, PeakTime provided independent information compared to AmpStd, otherwise no benefit would have arisen from combined deviation scores (Table 4, Fig. 6). It is unlikely that the effects observed in this study were due to neuropathy of the pupils or the efferent pathways, because there was no effect of absolute pupil size, and local defects were observed that were afferent (Fig. 3).

Afferent defects that could be driven by the cone-mediated yellow on-response of melanopsin-containing regional ganglion cells (mcRGCs) are interesting because those cells proceed directly to the pretectal olivary nucleus (PON).^{41,42} The PON is the main input to the Edinger-Westphal nucleus (EWN) on the efferent pathway to the pupils.⁴³ Thus, if this were the only input to the PON, the mfPOP response would largely be determined by retinal function. However, about half the input to the PON comes from other sources, mostly the extrastriate visual cortex.⁴³ Therefore, several cortically derived sources of luminance responses, including mcRGCs (about half of which go to the LGN),^{41,42} may contribute to the mfPOP responses. On balance, we cannot equate the observed afferent responses completely with retinal sources, although it is possible.

Asymmetry analysis has been shown to be useful in several mfVEP and mfERG studies⁴⁴⁻⁴⁶ and a similar result was obtained here. It is perhaps not surprising that a test comparing the two eyes of an individual can be more sensitive than comparisons against a normative database. Of course, the number of fields in this study, particularly in those with T2D for >10 years, was relatively small ($n = 32$), and so confirmatory studies are required. The ages of those patients were similar to those of all patients (Table 4), and thus they received the diagnosis at the age if ~ 47 years. Their mean A1c levels, $7.1\% \pm 0.90\%$, were similar to all patients, $7.1\% \pm 0.96\%$. Even though the actual onset might precede diagnosis by several years, these A1c levels and onset ages are reported to provide odds ratios of approximately 3 for DR.⁴⁷

Figure 2 shows that small signals can sometimes be obtained from some regions, which can be further affected by low signal-to-noise ratios (SNRs), occasionally (like any perimeter) providing false positives. We used a test time of 4 minutes. Extending the TrueField test time to 6 minutes for both eyes would still be about twice as fast as the Matrix and HFA II (both Carl Zeiss Meditec, Inc.) perimeters in patients,⁴⁸ and would provide about a 1.22 times ($\sqrt{6/4}$) improvement in SNR. Even at the 2 minutes per field of this study, the average effects of SNR were small, given that AUCs of approximately 95% were obtained. Subsequent improvements in the TrueField method have increased the response sizes in regions that

produced smaller responses in our study (Maddess T, et al. IOVS 2009;50:ARVO E-Abstract 5281).

A robust feature is our use of normalized pupil size, an approach that largely counteracts the effects of senescent pupils. Diabetes has been associated with pupillary autonomic denervation, and mean dark-adapted pupil size does appear appreciably smaller in diabetic patients.^{49,50} Note that there was no difference in the absolute pupil sizes of our study groups, and pupil size had no diagnostic power.

A mystery was that T2D seemed to produce larger than normal responses (Table 2), at least from peripheral regions (Fig. 4). One suggestion is that perhaps regulation of retinal function has been generally ramped up to assist central regions damaged by T2D. While depression of the SWAP MD^{7,11} has been reported for population means, inspection of individual data suggests that up to a quarter of subjects can have SWAP MDs from 0 to +4.5 dB,¹¹ whereas the mean effect in our study was +0.29 dB. MDs are calculated by applying reduced weight to peripheral TDs.⁵¹ In this study, response elevation was mainly peripheral and our stimulus regions extended to 30°, compared with 21° for many peripheral locations of the 24-2 field. An examination of peripheral TDs from 30-2 fields in T2D patients could well be revealing.

CONCLUSION

In a pilot study of sparse multifocal pupillography, the subset of our patients who had had T2D for at least 10 years gave AUCs as high as 95% for a test time of 2 minutes per eye.

References

1. Dunstan DW, Zimmet PZ, Welborn TA, et al. The rising prevalence of diabetes and impaired glucose tolerance: the Australian Diabetes, Obesity and Lifestyle Study. *Diabetes Care*. 2002;25:829-834.
2. Centers for Disease Control. *National Diabetes Fact Sheet*. U.S. Atlanta: Department of Human Services; 2005.
3. Stratton IM, Kohner EM, Aldington SJ, et al. UKPDS 50: risk factors for incidence and progression of retinopathy in type II diabetes over 6 years from diagnosis. *Diabetologia*. 2001;44:156-163.
4. Gardner TW, Antonetti DA, Barber AJ, LaNoue KF, Nakamura M. New insights into the pathophysiology of diabetic retinopathy: potential cell-specific therapeutic targets. *Diabetes Technol Ther*. 2000;2:601-608.
5. Trick GL, Trick LR, Kilo C. Visual field defects in patients with insulin-dependent and non-insulin-dependent diabetes. *Ophthalmology*. 1990;97:475-482.
6. Arend O, Remky A, Evans D, Stuber R, Harris A. Contrast sensitivity loss is coupled with capillary dropout in patients with diabetes. *Invest Ophthalmol Vis Sci*. 1997;30:1732-1737.
7. Afrashi F, Erakgun T, Kose S, Ardic K, Mentis J. Blue-on-yellow perimetry versus achromatic perimetry in type 1 diabetes patients without retinopathy. *Diabetes Res Clin Pract*. 2003;61:7-11.
8. Bengtsson B, Heijl A, Agardh E. Visual fields correlate better than visual acuity to severity of diabetic retinopathy. *Diabetologia*. 2005;48:2494-2500.
9. Stavrou EP, Wood JM. Central visual field changes using flicker perimetry in type 2 diabetes mellitus. *Acta Ophthalmol Scand*. 2005;83:574-580.
10. Agardh E, Stjernquist H, Heijl A, Bengtsson B. Visual acuity and perimetry as measures of visual function in diabetic macular oedema. *Diabetologia*. 2006;49:200-206.
11. Nitta K, Saito Y, Kobayashi A, Sugiyama K. Influence of clinical factors on blue-on-yellow perimetry for diabetic patients without retinopathy. *Retina*. 2006;26:797-802.
12. Birt CM, Shin DH, Samudrala V, Hughes BA, Kim C, Lee D. Analysis of reliability indices from Humphrey visual field tests in an urban glaucoma population. *Ophthalmology*. 1997;104:1126-1130.
13. Ivers RQ, Macaskill P, Cumming RG, Mitchell P. Sensitivity and specificity of tests to detect eye disease in an older population. *Ophthalmology*. 2001;108:968-975.

14. Pierre-Filho PTP, Schimitti RB, de Vasconcellos JPC, Costa VP. Sensitivity and specificity of frequency-doubling technology, tendency-oriented perimetry, SITA Standard and SITA Fast perimetry in perimetrically inexperienced individuals. *Acta Ophthalmol Scand*. 2006;84:345-350.
15. Keltner JL, Johnson CA, Beck RW, Cleary PA, Spurr JO. Quality control functions of the Visual Field Reading Center (VFRC) for the Optic Neuritis Treatment Trial (ONTT). *Control Clin Trials*. 1993;14:143-159.
16. Carpineto P, Ciancaglini M, Di Antonio L, Gavalas C, Mastropasqua L. Fundus micropertimetry patterns of fixation in type 2 diabetic patients with diffuse macular edema. *Retina*. 2007;27:21-29.
17. Sutter E, Tran D. The field topography of ERG components in man, I. The photopic luminance response. *Vision Res*. 1992;32:433-446.
18. Bearse MA, Adams AJ, Han Y, et al. A multifocal electroretinogram model predicting the development of diabetic retinopathy. *Prog Retin Eye Res*. 2006;25:425-448.
19. Kurtenbach A, Langrova H, Zrenner E. Multifocal oscillatory potentials in type 1 diabetes without retinopathy. *Invest Ophthalmol Vis Sci*. 2000;41:3234-3241.
20. Bronson-Castain KW, Bearse MA Jr, Han Y, Schneck ME, Barez S, Adams AJ. Association between multifocal ERG implicit time delays and adaptation in patients with diabetes. *Invest Ophthalmol Vis Sci*. 2007;48:5250-5266.
21. Ng J, Bearse MA, Schneck ME, Barez S, Adams AJ. Local diabetic retinopathy prediction by multifocal ERG delays over 3 years. *Invest Ophthalmol Vis Sci*. 2008;49:1622-1628.
22. James AC. The pattern-pulse multifocal visual evoked potential. *Invest Ophthalmol Vis Sci*. 2003;44:879-890.
23. James AC, Ruseckaite R, Maddess T. Effect of temporal sparseness and dichoptic presentation on multifocal visual evoked potentials. *Vis Neurosci*. 2005;22:45-54.
24. Maddess T, James AC, Bowman EA. Contrast response of temporally sparse dichoptic multifocal visual evoked potentials. *Vis Neurosci*. 2005;22:153-162.
25. Maddess T, James AC, Ruseckaite R, Bowman EA. Hierarchical decomposition of dichoptic multifocal visual evoked potentials. *Vis Neurosci*. 2006;23:703-712.
26. Arvind H, Klistorner A, Graham S, et al. Multifocal visual evoked responses to dichoptic stimulation using virtual reality goggles: multifocal VER to dichoptic stimulation. *Doc Ophthalmol*. 2006;112:189-199.
27. Ruseckaite R, Maddess T, Danta G, Lueck CJ, James AC. Sparse multifocal stimuli for the detection of multiple sclerosis. *Ann Neurol*. 2005;57:904-913.
28. Arvind H, Klistorner A, Graham S, et al. Dichoptic stimulation improves detection of glaucoma with multifocal visual evoked potentials. *Invest Ophthalmol Vis Sci*. 2007;48:4590-4596.
29. Bjerre A, Grigg JR, Parry NR, Henson DB. Test-retest variability of multifocal visual evoked potential and SITA standard perimetry in glaucoma. *Invest Ophthalmol Vis Sci*. 2004;45:4035-4040.
30. Kardon RH, Kirkali PA, Thompson HS. Automated pupil perimetry: pupil field mapping in patients and normal subjects. *Ophthalmology*. 1991;98:485-495; discussion 495-496.
31. Hong S, Narkiewicz J, Kardon RH. Comparison of pupil perimetry and visual perimetry in normal eyes: decibel sensitivity and variability. *Invest Ophthalmol Vis Sci*. 2001;42:957-965.
32. Tan L, Kondo M, Sato M, Kondo N, Miyake Y. Multifocal pupillary light response fields in normal subjects and patients with visual field defects. *Vision Res*. 2001;41:1073-1084.
33. Wilhelm H, Neitzel J, Wilhelm B, et al. Pupil perimetry using M-sequence stimulation technique. *Invest Ophthalmol Vis Sci*. 2000;41:1229-1238.
34. Maddess T, Bedford S, Goh XL, James AC. Multifocal pupillo-graphic visual field testing in glaucoma. *Clin Exp Ophthalmol*. 2009;37:678-686.
35. James AC, Maddess T. Method and apparatus for assessing neural function by sparse stimuli. Australia Patent No. PQ 6465-00. 2000.
36. Lee YW, Schetzen M. Measurement of Wiener kernels of a non-linear system by cross-correlation. *Int J Control*. 1965;2:237-254.
37. Hanley JA, McNeil BJ. The meaning and use of the area under a receiver operating characteristic (ROC) curve. *Radiology*. 1982;143:29-36.
38. Johnson RA, Wichern DW. *Applied Multivariate Statistical Analysis*. 3rd ed. Englewood Cliffs, NJ: Prentice Hall; 1992.
39. Fawcett T. An introduction to ROC analysis. *Pattern Recogn Lett*. 2006;27:861-874.
40. Fletcher EL, Phipps JA, Ward MM, et al. Neuronal and glial cell abnormality as predictors of progression of diabetic retinopathy. *Curr Pharm Design*. 2007;13:2699-2712.
41. Dacey DM, Liao HW, Peterson BB, et al. Melanopsin-expressing ganglion cells in primate retina signal colour and irradiance and project to the LGN. *Nature*. 2005;433:749-754.
42. Dacey DM, Peterson BB, Robinson FR, Gamlin PD. Fireworks in the primate retina: in vitro photodynamics reveals diverse LGN-projecting ganglion cell types. *Neuron*. 2003;37:15-27.
43. Gamlin PD. The pretectum: connections and oculomotor-related roles. *Prog Brain Res*. 2006;151:379-405.
44. Graham SL, Klistorner AI, Grigg JR, Billson FA. Objective VEP perimetry in glaucoma: asymmetry analysis to identify early deficits. *J Glaucoma*. 2000;9:10-19.
45. Fortune B, Bearse MA Jr, Cioffi GA, Johnson CA. Selective loss of an oscillatory component from temporal retinal multifocal ERG responses in glaucoma. *Invest Ophthalmol Vis Sci*. 2002;43:2638-2647.
46. Hood DC, Zhang X, Rodarte C, et al. Determining abnormal interocular latencies of multifocal visual evoked potentials. *Doc Ophthalmol*. 2004;109:177-187.
47. Wong J, Molyneux L, Constantino M, Twigg SM, Yue DK. Timing is everything: age of onset influences long-term retinopathy risk in type 2 diabetes, independent of traditional risk factors. *Diabetes Care*. 2008;31:1985-1990.
48. Sakata LM, Deleon-Ortega J, Arthur SN, Monheit BE, Girkin CA. Detecting visual function abnormalities using the Swedish interactive threshold algorithm and matrix perimetry in eyes with glaucomatous appearance of the optic disc. *Arch Ophthalmol*. 2007;125:340-345.
49. Cahill M, Eustace P, de Jesus V. Pupillary autonomic denervation with increasing duration of diabetes mellitus. *Br J Ophthalmol*. 2001;85:1225-1230.
50. Pittasch D, Behrans-Baumann W, Lobmann R, Lowe SW. Pupil signs of sympathetic autonomic neuropathy in patients with type 1 diabetes. *Diabetes Care*. 2002;25:1545-1550.
51. Anderson D. *Automated Static Perimetry*. St. Louis: Mosby Year Book; 1992.